

Voltage Profile Improvement and Power Loss Reduction on the Nigeria 330 kV Power Transmission System using Unified Power Flow Controller (UPFC)

Onah, C.O.¹, Kpochi, P. K.² and Idoko, E.³

^{1, 2, 3}Department of Electrical and Electronics Engineering, Federal University of Agriculture, Makurdi, Nigeria

-----ABSTRACT-----

This paper presents the power flow analysis of the Nigeria 330 kV, 34-bus transmission network under steady-state and under the application of a Flexible Alternating Current Transmission System (FACTS) device - Unified Power Flow Controller (UPFC). The modeling and simulations required for a thorough study of the steady-state operation of the electric power system with UPFC are presented in detail. The analysis of the system model was performed using the NEPLAN software environment and the simulation results of the 34-bus system before and after the introduction of UPFC are equally presented. Results from the analysis revealed that before the incorporation of UPFC, seven (7) buses of the thirty-four (34) buses of the case study have their voltage magnitudes outside the acceptable value limit of $313.5 \leq V \leq 346.5$ kV., which were improved to 330 kV each at the introduction of UPFC. Also, the active power loss was reduced by 11.67%. Thus, the application of UPFC on the Nigeria 330 kV power system network stabilizes the system's voltage and causes a reduction in the total power loss, which attests to an improvement in the power system performance.

Keywords: Power Flow Analysis, FACTS, UPFC, Steady-state, Real and Reactive Power, NEPLAN

Date of Submission: 12-06-2024

Date of acceptance: 24-06-2024

I. INTRODUCTION

The demand for electrical energy around the world increases daily. The ever-growing need for the transmission of more electrical power can be met either by installing new transmission lines or by using the existing ones in a more efficient way. The construction of new transmission lines is increasingly difficult due to several reasons, such as regulatory, environmental, and public policies, as well as the ever-increasing cost. The power industry is in constant pursuit of the most economic ways to transmit bulk power along a desired path. Before considering new transmission lines, it is desirable to explore other ways to increase the usage of existing transmission lines by increasing their power flow [1-3]. While the power flow in some of these transmission lines is well below their thermal limits, certain lines are overloaded, which has the effect of deteriorating voltage profiles and decreasing system stability. This requires the assessment of traditional transmission methods and practices, and the creation of new concepts to allow for the use of existing transmission systems without a reduction in system security [4].

Consequently, it is envisaged that a new solution to such operational problems will rely on the upgrading of existing transmission corridors by using the latest power electronic equipment and methods, a new technological thinking that comes under the generic title of FACTS – an acronym for flexible alternating current transmission systems [5-7]. FACTS technology is a new approach taking advantage of the advances in power electronics controllers for enhancing the existing power system infrastructures [8-10]. FACTS permits an improvement in transmission system operation and control with reduced infrastructure investment, environmental impact, and implementation time, increase system security and reliability, increase power transfer capabilities, and enhancement in the quality of the electrical energy delivered at the receiving end [11]. Several categories of FACTS controllers are in use and the most prevalent types are Interphase Power Controller (IPC), Generalized Unified Power Flow Controller (GUPFC), Static Synchronous Compensator (STATCOM), Static Var Compensator (SVC), Thyristor Controlled Breaking Reactor (TCR), Thyristor Controlled Series Capacitor (TCSC), Static Synchronous Series Compensator (SSSC), Interline Power Flow Controller (IPFC), Thyristor Switched Series Reactor (TSSR), Unified Power Flow Controller (UPFC) [12]. Each of these categories of FACTS devices has certain peculiarities, which can be deployed for different applications and on this basis, several studies have been conducted to investigate the potential applications and benefits arising from their applications [10 - 12].

In this paper, the focus is to study the impact of a Unified Power Flow Controller (UPFC) on the transmission system network using the Nigeria 330 kV, 34-bus Power System as a case study. UPFC is considered a universal tool for power flow control due to its ability to simultaneously and independently control all three system parameters, which affect power flow, i.e. terminal voltage, transmission angle and system reactance [12].

II. UNIFIED POWER FLOW CONTROLLER

2.1 Basic Concept of UPFC

The basic model of UPFC is as depicted in Fig.1. It comprises the Static Synchronous Compensator (STATCOM) and the static synchronous series compensator (SSSC) with a shared DC link. The SSSC injects a compensating voltage $V_{s's}$ that is at any phase angle with the prevailing line current I . The series-connected compensating voltage $V_{s's}$ has active and reactive components, which are V_d and V_q with load convention. The component V_d of the compensating voltage that is either in phase or out of phase with the line current emulates a positive or a negative resistor in series with the line. The remaining component V_q that is in quadrature with the line current emulates either an inductor or a capacitor in series with the transmission line [1]. The compensating voltage $V_{s's}$ exchanges active and reactive powers P_{exch} and Q_{exch} that are defined as equations (1) and (2) respectively.

$$P_{exch} = -V_{s's} * I = V_{dq} I = V_d I = V_s I_d \quad (1)$$

$$Q_{exch} = |-V_{s's} \times I| = |V_{dq} \times I| = V_q \quad (2)$$

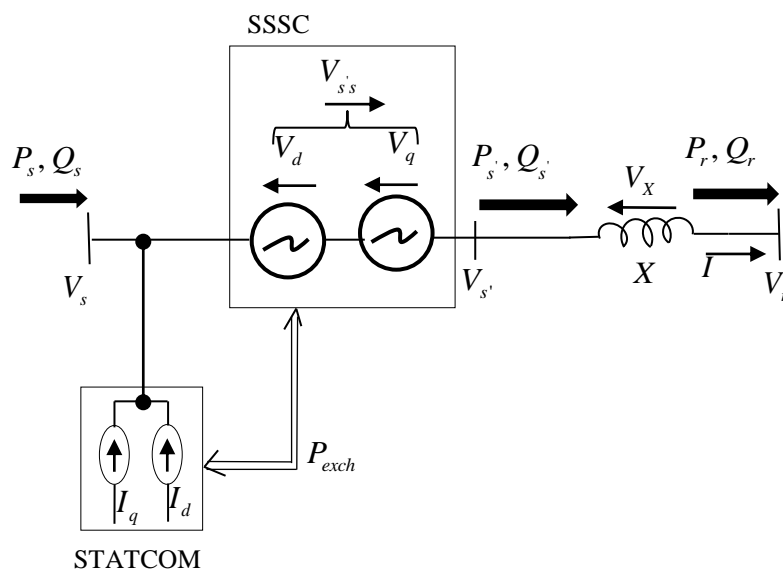


Fig. 1 Basic Model of the Unified Power Flow Controller [1]

2.2 Power Flow Model of UPFC

The equivalent circuit of Fig. 2, which consists of two coordinated synchronous voltage sources, is used to represent the UPFC adequately for the purpose of fundamental frequency steady-state analysis. The synchronous voltage sources represent the fundamental Fourier series component of the switched voltage waveforms at the AC converter terminals of the UPFC [11].

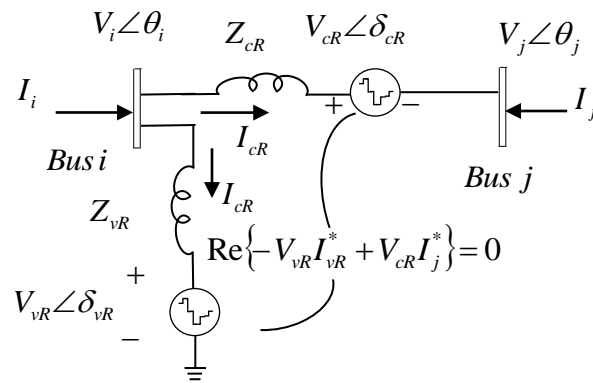


Fig. 2 Equivalent Circuit of Unified Power Flow Controller

The voltage sources of the unified power flow controller are described by equations (3) and (4).

$$E_{vR} = V_{vR} (\cos \delta_{vR} + j \sin \delta_{vR}) \quad (3)$$

$$E_{cR} = V_{cR} (\cos \delta_{cR} + j \sin \delta_{cR}) \quad (4)$$

where V_{vR} and δ_{vR} defined the controllable magnitude in the range, $V_{vR \min} \leq V_{vR} \leq V_{vR \max}$ and phase angle ($0 \leq \delta_{vR} \leq 2\pi$) of the voltage source representing the shunt converter, V_{cR} and δ_{cR} are the magnitude and the phase angle of the voltage source representing the series converter, which are controllable between limits ($V_{cR \min} \leq V_{cR} \leq V_{cR \max}$) and ($0 \leq \delta_{cR} \leq 2\pi$) respectively.

The mode of power flow control is highly dependent on the phase angle of the series-injected voltage. The terminal voltage is regulated by the UPFC if δ_{cR} is in phase with the nodal voltage angle θ_i . But if δ_{cR} is in quadrature with respect to θ_i , it controls active power flow, acting as a phase shifter. On the other hand, if δ_{cR} is in quadrature with the line current angle, then it controls active power flow acting as a variable series compensator. At any other value of δ_{cR} , the operation of UPFC is a combination of voltage regulator, variable series compensator, and phase shifter. The capacity of power flow to be controlled is a function of the magnitude of the series-injected voltage [11, 12].

From the equivalent circuit depicted in Fig. 2 and equations (3) and (4), the active and reactive power equations at bus i are given by equations (5) and (6) [11].

$$P_i = V_i^2 G_{ii} + V_i V_j [G_{ij} \cos(\theta_i - \theta_j) + B_{ij} \sin(\theta_i - \theta_j)] + V_i V_{cR} [G_{ij} \cos(\theta_i - \delta_{cR}) + B_{ij} \sin(\theta_i - \delta_{cR})] + V_i V_{vR} [G_{vR} \cos(\theta_i - \delta_{vR}) + B_{vR} \sin(\theta_i - \delta_{vR})] \quad (5)$$

$$Q_i = -V_i^2 B_{ii} + V_i V_j [G_{ij} \sin(\theta_i - \theta_j) - B_{ij} \cos(\theta_i - \theta_j)] + V_i V_{cR} [G_{ij} \sin(\theta_i - \delta_{cR}) + B_{ij} \cos(\theta_i - \delta_{cR})] + V_i V_{vR} [G_{vR} \sin(\theta_i - \delta_{vR}) - B_{vR} \cos(\theta_i - \delta_{vR})] \quad (6)$$

Similarly, the active and reactive power equations at bus j can be obtained as given by equations (7) and (8).

$$P_j = V_j^2 G_{jj} + V_j V_i [G_{ji} \cos(\theta_j - \theta_i) + B_{ji} \sin(\theta_j - \theta_i)] + V_j V_{cR} [G_{jj} \cos(\theta_j - \delta_{cR}) + B_{jj} \sin(\theta_j - \delta_{cR})] \quad (7)$$

$$Q_j = -V_j^2 B_{jj} + V_j V_i [G_{ji} \sin(\theta_i - \theta_j) - B_{ji} \cos(\theta_j - \theta_i)] + V_j V_{cR} [G_{jj} \sin(\theta_j - \delta_{cR}) - B_{jj} \cos(\theta_j - \delta_{cR})] \quad (8)$$

The active and reactive power of the series converter, are also given by equations (9) and (10).

$$P_{cR} = V_{cR}^2 G_{jj} + V_{cR} V_i [G_{ij} \cos(\delta_{cR} - \theta_i) + B_{ij} \sin(\delta_{cR} - \theta_i)] + V_{cR} V_j [G_{jj} \cos(\delta_{cR} - \theta_j) + B_{jj} \sin(\delta_{cR} - \theta_j)] \quad (9)$$

$$Q_{cR} = -V_{cR}^2 B_{jj} + V_{cR} V_i \left[G_{ij} \sin(\delta_{cR} - \theta_i) - B_{ij} \cos(\delta_{cR} - \theta_i) \right] + V_{cR} V_j \left[G_{jj} \sin(\delta_{cR} - \theta_j) - B_{jj} \cos(\delta_{cR} - \theta_j) \right] \quad (10)$$

Representing the active and reactive power expressions of the shunt converters are equations (11) and (12).

$$P_{vR} = -V_{vR}^2 G_{vR} + V_{vR} V_i \left[G_{vR} \cos(\delta_{vR} - \theta_i) + B_{vR} \sin(\delta_{cR} - \theta_i) \right] \quad (11)$$

$$Q_{vR} = V_{cR}^2 B_{vR} + V_{vR} V_i \left[G_{vR} \sin(\delta_{vR} - \theta_i) - B_{vR} \cos(\delta_{cR} - \theta_i) \right] \quad (12)$$

In the voltage sources model considered, the UPFC converters are assumed to be loss-less converter valves, which implies that the active power supplied to the shunt converter, P_{vR} , equals the active power demanded by the series converter, P_{cR} as described by equation (13).

$$P_{vR} + P_{cR} = 0 \quad (13)$$

Also, if the coupling transformers are assumed to contain no resistance then the active power at bus i matches the active power at bus j; consequently, it can be expressed as equation (14).

$$P_{vR} + P_{cR} = P_i + P_j = 0 \quad (14)$$

In linearized form, the UPFC power equations are combined with AC network. In a situation when the UPFC controls parameters such as voltage magnitude at the shunt converter terminal (bus i), active power flow from bus j to bus i, and reactive power injected at bus j, and taking bus j to be a PQ bus, the linearized system of equation is given by the matrix of equation (15).

$$\begin{bmatrix} \Delta P_i \\ \Delta P_j \\ \Delta Q_i \\ \Delta Q_j \\ \Delta P_{ji} \\ \Delta Q_{ji} \\ \Delta P_{bb} \end{bmatrix} = \begin{bmatrix} \frac{\partial P_i}{\partial \theta_i} & \frac{\partial P_i}{\partial \theta_j} & \frac{\partial P_i}{\partial V_{vR}} V_{vR} & \frac{\partial P_i}{\partial V_j} V_j & \frac{\partial P_i}{\partial \delta_{cR}} & \frac{\partial P_i}{\partial V_{cR}} V_{cR} & \frac{\partial P_i}{\partial \delta_{vR}} \\ \frac{\partial P_j}{\partial \theta_i} & \frac{\partial P_j}{\partial \theta_j} & 0 & \frac{\partial P_j}{\partial V_j} V_j & \frac{\partial P_j}{\partial \delta_{cR}} & \frac{\partial P_j}{\partial V_{cR}} V_{cR} & 0 \\ \frac{\partial Q_i}{\partial \theta_i} & \frac{\partial Q_i}{\partial \theta_j} & \frac{\partial Q_i}{\partial V_{vR}} V_{vR} & \frac{\partial Q_i}{\partial V_j} V_j & \frac{\partial Q_i}{\partial \delta_{cR}} & \frac{\partial Q_i}{\partial V_{cR}} V_{cR} & \frac{\partial Q_i}{\partial \delta_{vR}} \\ \frac{\partial Q_j}{\partial \theta_i} & \frac{\partial Q_j}{\partial \theta_j} & 0 & \frac{\partial Q_j}{\partial V_j} V_j & \frac{\partial Q_j}{\partial \delta_{cR}} & \frac{\partial Q_j}{\partial V_{cR}} V_{cR} & 0 \\ \frac{\partial P_{ji}}{\partial \theta_i} & \frac{\partial P_{ji}}{\partial \theta_j} & 0 & \frac{\partial P_{ji}}{\partial V_j} V_j & \frac{\partial P_{ji}}{\partial \delta_{cR}} & \frac{\partial P_{ji}}{\partial V_{cR}} V_{cR} & 0 \\ \frac{\partial Q_{ji}}{\partial \theta_i} & \frac{\partial Q_{ji}}{\partial \theta_j} & 0 & \frac{\partial Q_{ji}}{\partial V_j} V_j & \frac{\partial Q_{ji}}{\partial \delta_{cR}} & \frac{\partial Q_{ji}}{\partial V_{cR}} V_{cR} & 0 \\ \frac{\partial P_{bb}}{\partial \theta_i} & \frac{\partial P_{bb}}{\partial \theta_j} & \frac{\partial P_{bb}}{\partial V_{vR}} V_{vR} & \frac{\partial P_{bb}}{\partial V_j} V_j & \frac{\partial P_{bb}}{\partial \delta_{cR}} & \frac{\partial P_{bb}}{\partial V_{cR}} V_{cR} & \frac{\partial P_{bb}}{\partial \delta_{vR}} \end{bmatrix} \begin{bmatrix} \Delta \theta_i \\ \Delta \theta_j \\ \frac{\Delta V_{vR}}{V_{vR}} \\ \frac{\Delta V_j}{V_j} \\ \Delta \delta_{cR} \\ \frac{\Delta V_{cR}}{V_{cR}} \\ \Delta \delta_{vR} \end{bmatrix} \quad (15)$$

where ΔP_{bb} is the power mismatch given by equation (13).

In a condition when the voltage control atith bus is deactivated, the third column of equation (13) can be replaced by partial derivatives of the bus and UPFC mismatch powers with respect to the bus voltage magnitude V_i . Furthermore, the term $\Delta V_{vR}/V_{vR}$ that is the voltage magnitude increment of the shunt source can be replaced by the voltage magnitude increment at ith bus, $\Delta V_i/V_i$. Thus, taking buses i and j as PQ buses, the linearized system of equations is as given by equation (16).

$$\begin{bmatrix} \Delta P_i \\ \Delta P_j \\ \Delta Q_i \\ \Delta Q_j \\ \Delta P_{ji} \\ \Delta Q_{ji} \\ \Delta P_{bb} \end{bmatrix} = \begin{bmatrix} \frac{\partial P_i}{\partial \theta_i} & \frac{\partial P_i}{\partial \theta_j} & \frac{\partial P_i}{\partial V_i} V_i & \frac{\partial P_i}{\partial V_j} V_j & \frac{\partial P_i}{\partial \delta_{cR}} & \frac{\partial P_i}{\partial V_{cR}} V_{cR} & \frac{\partial P_i}{\partial \delta_{vR}} \\ \frac{\partial P_j}{\partial \theta_i} & \frac{\partial P_j}{\partial \theta_j} & \frac{\partial P_j}{\partial V_i} V_i & \frac{\partial P_j}{\partial V_j} V_j & \frac{\partial P_j}{\partial \delta_{cR}} & \frac{\partial P_j}{\partial V_{cR}} V_{cR} & 0 \\ \frac{\partial Q_i}{\partial \theta_i} & \frac{\partial Q_i}{\partial \theta_j} & \frac{\partial Q_i}{\partial V_i} V_i & \frac{\partial Q_i}{\partial V_j} V_j & \frac{\partial Q_i}{\partial \delta_{cR}} & \frac{\partial Q_i}{\partial V_{cR}} V_{cR} & \frac{\partial Q_i}{\partial \delta_{vR}} \\ \frac{\partial Q_j}{\partial \theta_i} & \frac{\partial Q_j}{\partial \theta_j} & \frac{\partial Q_j}{\partial V_i} V_i & \frac{\partial Q_j}{\partial V_j} V_j & \frac{\partial Q_j}{\partial \delta_{cR}} & \frac{\partial Q_j}{\partial V_{cR}} V_{cR} & 0 \\ \frac{\partial P_{ji}}{\partial \theta_i} & \frac{\partial P_{ji}}{\partial \theta_j} & \frac{\partial P_{ji}}{\partial V_i} V_i & \frac{\partial P_{ji}}{\partial V_j} V_j & \frac{\partial P_{ji}}{\partial \delta_{cR}} & \frac{\partial P_{ji}}{\partial V_{cR}} V_{cR} & 0 \\ \frac{\partial Q_{ji}}{\partial \theta_i} & \frac{\partial Q_{ji}}{\partial \theta_j} & \frac{\partial Q_{ji}}{\partial V_i} V_i & \frac{\partial Q_{ji}}{\partial V_j} V_j & \frac{\partial Q_{ji}}{\partial \delta_{cR}} & \frac{\partial Q_{ji}}{\partial V_{cR}} V_{cR} & 0 \\ \frac{\partial P_{bb}}{\partial \theta_i} & \frac{\partial P_{bb}}{\partial \theta_j} & \frac{\partial P_{bb}}{\partial V_i} V_i & \frac{\partial P_{bb}}{\partial V_j} V_j & \frac{\partial P_{bb}}{\partial \delta_{cR}} & \frac{\partial P_{bb}}{\partial V_{cR}} V_{cR} & \frac{\partial P_{bb}}{\partial \delta_{vR}} \end{bmatrix} \begin{bmatrix} \Delta \theta_i \\ \Delta \theta_j \\ \frac{\Delta V_i}{V_i} \\ \frac{\Delta V_j}{V_j} \\ \Delta \delta_{cR} \\ \frac{\Delta V_{cR}}{V_{cR}} \\ \Delta \delta_{vR} \end{bmatrix} \quad (16)$$

Here, the controllable voltage magnitude, V_{vR} is maintained at a fixed value within prescribed limits, $V_{vR \min} \leq V_{vR} \leq V_{vR \max}$

III. RESULTS AND DISCUSSION

The results of the power flow simulation performed on the Nigeria 330 kV, 34-bus power system network both for steady-state and during the introduction of UPFC are presented in this section. All the relevant data utilized in the simulation and analyses of the case study in this paper were obtained from the Transmission Company of Nigeria Control Centre, Osogbo [13]. The 34-bus network shown in Fig. 3 consists of thirty-four (34) buses, nine (9) generation stations, and fifty-two (52) transmission lines. The bus data and transmission line data are shown in Tables 1 and 2 respectively. While Table 3 represents the steady-state power flow results of the Nigeria 330 kV 34-Bus power system.

Under the steady-state conditions, the total active power loss was found to be 43.59 MW, while the total reactive power loss was -538.56 MVar. Seven buses, which were found to have their bus voltages below acceptable values include Kano 305.097 kV, New Haven 313.249 kV, Kaduna 309.721 kV, Jos 305.563 kV, Makurdi 304.787 kV, Gombe 304.443 kV and Yola 300.375 kV.

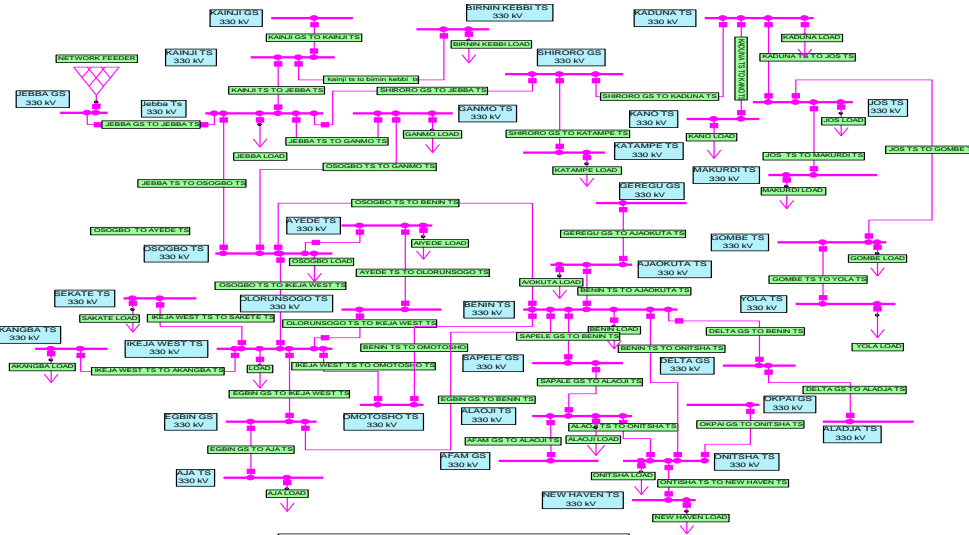


Fig. 3 Load Flow of the Nigeria 330 kV, 34-bus Power System

Table 1: Load Data of the Nigeria 330 kV, 34-Bus Power System [13]

S/N	BUS INTERCONNECTIVITY		LENGTH (KM)	No of line(s)	RESISTANCE (P.U)	REACTANCE (P.U)	SHUNT (y/2) P.U
	FROM	TO					
1	B. KEBBI T.S	KAINJI T.S	310	1	0.011102	0.094224	1.17723
3	KAINJI T.S	JEBBA T.S	81	2	0.002901	0.02462	0.3076
4	JEBBA G.S	JEBBA T.S	8	2	0.000289	0.00223	0.03312
5	JEBBA T.S	SHIRORO G.S	244	2	0.008738	0.074163	0.9266
6	JEBBA T.S	GANMO T.S	70	1	0.003939	0.013343	0.41842
7	GANMO T.S	OSOGBO T.S	87	1	0.001683	0.014286	0.17848
8	JEBBA T.S	OSOGBO T.S	157	2	0.005623	0.04772	0.59621
9	KADUNA T.S	KANO T.S	230	1	0.008237	0.069908	0.87343
10	KADUNA T.S	SHIRORO G. S	95	2	0.003438	0.074163	0.36456
11	KADUNA T.S	JOS T.S	197	1	0.007019	0.059574	0.74432
12	SHIRORO	KATAMPE	144	1	0.007887	0.060656	0.90244
13	JOS T.S	MAKURDI T.S	285	2	0.002876	0.024557	0.00323
14	JOS T.S	GOMBE T.S	265	1	0.009455	0.080242	1.00255
15	GOMBE T.S	YOLA T.S	240	1	0.008595	0.072948	0.91141
16	AJAOKUTA T.S	GEREGU G.S	75	2	0.000036	0.000278	0.00414
17	AJAOKUTA T.S	BENIN T.S	195	2	0.007055	0.054256	0.80723
18	N/HAVEN T.S	ONITSHA T.S	96	1	0.003438	0.029179	0.36456
19	ONITSHA T.S	OKPAI P.S	56	2	0.002171	0.016674	0.24838
20	ONITSHA	ALAOJI T.S	138	1	0.004942	0.041945	0.52406
21	ALAOJI T.S	AFAM	25	2	0.000905	0.006956	0.10349
22	BENIN T.S	ONITSHA T.S	137	2	0.004906	0.041641	0.52026
23	BENIN T.S	SAPELE G.S	50	3	0.001809	0.013912	0.20698
24	SAPELE	ALAOJI	93	1	0.002256	0.019149	0.23924
25	BENIN	DELTA G.S	107	1	0.001468	0.012462	0.1577
26	DELTA G.S	ALADJA	30	1	0.001146	0.009726	0.12152
27	OSOGBO T.S	AYEDE T.S	119	1	0.004118	0.034954	0.43672
28	AYEDE T.S	OLORUNSOGO	60	1	0.002149	0.018237	0.22785

29	OLORUNSOGO	IKEJA WEST T.S	77	1	0.002757	0.023403	0.29239
30	BENIN T.S	EGBIN G.S	218	1	0.007163	0.06079	0.75951
31	BENIN T.S	OMOTOSHO	120	1	0.00286	0.024336	0.41842
32	OMOTOSHO	IKEJA WEST	160	1	0.00716	0.060787	0.75947
33	SAKETE	IKEJA WEST	70	1	0.002507	0.021276	0.26583
34	AKANGBA	IKEJA WEST	18	2	0.000615	0.00437	0.07037
35	IKEJA WEST	EGBIN G.S	15.2	1	0.000645	0.005471	0.06836
36	AJA T.S	EGBIN G.S	14	2	0.000501	0.004255	0.05317
37	OSOGBO T.S	BENIN T.S	251	1	0.008989	0.076291	0.95318
38	IKEJA WEST	OSOGBO	250	1	0.008953	0.075987	0.94938

Table 2: Transmission Line Parameters of the Nigeria 330 kV, 34-Bus Power System [13]

S/N	BUS NAME	P(MW)	Q(MVAR)	Voltage (kV)
1	IKEJA WEST	420	85	315
2	KADUNA	300	45	315
3	KANO	300	45	300
4	YOLA	120	20	317
5	JOS	100	20	324
6	GOMBE	80	20	305
7	SHIRORO	160	17	328
8	AIYEDE	120	33	335
9	OSOGBO	180	40	334
10	GANMO	80	45	335
11	BENIN	160	38	333
12	ONITSHA	160	40	329
13	ALAOJI	180	36	323
14	NEW HAVEN	120	38	331
15	JEBBA	60	20	338
16	BIRNIN KEBBI	110	40	329
17	SAKATE	180	53	311
18	KATAMPE	200	55	323
19	AKANGBA	120	45	331
20	MAKURDI	50	16	327
21	GWAGWALADA			327
22	AJA	100	25	313
23	ADIABOR			
24	IKOT EKPENE			327
25	UGWUAJI			336
26	LOKOJA			332
27	LEKKI TS			N/R
28	ALAGBON T.S			N/R
29		40	20	340

The simulation of the Nigeria 330 kV, 34-bus of the power system was successfully performed using NEPLAN software under the conditions of steady-state and the introduction of UPFC. Under the steady-state conditions as

shown in Table 3, the total real power loss was found to be 43,59 MW, while that of reactive power loss was - 538.56 MVar. But at the introduction of UPFC at the various buses with voltage magnitudes outside acceptable limit, the results are as presented in Table 4, Fig. 4 and Fig. 5.

Fig. 4 depicts the plot of voltage magnitude against buses of the power system network before and after the introduction of UPFC, which revealed that there was an improvement in the voltage profile of the buses 19 (Kano), 26 (New Haven), 30 (Jos), 31 (Kaduna), 32 (Gombe), 33 (Makurdi) and 34 (Yola) due to the introduction of UPFC.

Fig. 5 shows the total real power loss before and after the compensation. The result shows a reduction of 9.4% in total reactive power loss from 49.35 MW to 43.59 MW, which signifies an improvement in the active power transmission capacity of the transmission lines. These results of the analysis indicate that UPFC is capable of improving the voltage at buses and also reducing system power loss on the power system network.

Table 3: Steady State Power Flow Results of the Nigeria 34 Bus 330 kV Power System

S/N	Bus Name	U kV	u %	Angle U °	P Load MW	Q Load MVar
1	KATAMPE TS	312.488	94.69	-6.6	200	55
2	KAINJI GS	329.784	99.93	-0.1	0	0
3	AJA TS	316.219	95.82	-5.3	100	25
4	KAINJI TS	329.784	99.93	-0.1	0	0
5	AYEDE TS	319.803	96.91	-3.7	120	33
6	BIRNIN KEBBI TS	324.886	98.45	-1.7	110	40
7	OLORUNSOGO TS	318.43	96.49	-4.3	0	0
8	Jebba Ts	329.956	99.99	0	60	20
9	BENIN TS	314.508	95.31	-6.1	160	38
10	ALAOJI TS	314.179	95.21	-6.2	180	36
11	SAPELE GS	314.413	95.28	-6.1	0	0
12	ONITSHA TS	313.716	95.07	-6.4	160	40
13	AFAM GS	314.179	95.21	-6.2	0	0
14	JEBBA GS	330	100	0	0	0
15	OKPAI GS	313.716	95.07	-6.4	0	0
16	GEREGU GS	314.083	95.18	-6.2	0	0
17	AJAOKUTA TS	314.083	95.18	-6.2	40	20
18	OSOGBO TS	326.002	98.79	-1.3	180	40
19	KANO TS	303.675	92.02	-12.4	300	45
20	ALADJA TS	314.508	95.31	-6.1	0	0
21	DELTA GS	314.508	95.31	-6.1	0	0
22	GANMO TS	327.801	99.33	-0.6	80	45
23	OMOTOSHO TS	314.904	95.43	-5.9	0	0
24	EGBIN GS	316.223	95.83	-5.3	0	0
25	IKEJA WEST TS	316.243	95.83	-5.3	420	85
26	NEW HAVEN TS	313.248	94.92	-6.6	120	38
27	AKANGBA TS	316.236	95.83	-5.3	120	45
28	SHIRORO GS	314.799	95.39	-5.6	0	0
29	SEKATE TS	315.892	95.72	-5.5	180	53
30	JOS TS	303.192	91.88	-12	100	20
31	KADUNA TS	308.324	93.43	-9.5	300	45
32	GOMBE TS	300.762	91.14	-13.3	80	20
33	MAKURDI TS	302.939	91.8	-12.1	50	16

34	YOLA TS	298.682	90.51	-14.6	120	20
Power Loss:		P= 49.36 MW	Q= 410.23 Mvar			

Table 4: Power Flow Results of the Nigeria330 kV, 34-Bus Power System with UPFC

S/N	BusName	U(kV)	u (%)	Angle U (°)	P Load (MW)	Q Load (MVar)
1	KATAMPE TS	324.883	98.45	-6.6	200	55
2	KAINJI GS	329.978	99.99	-0.1	0	0
3	AJA TS	324.206	98.24	-5.4	100	25
4	KAINJI TS	329.978	99.99	-0.1	0	0
5	AYEDE TS	325.328	98.58	-3.8	120	33
6	BIRNIN KEBBI TS	330	100	-1.8	110	40
7	OLORUNSOGO TS	324.872	98.45	-4.4	0	0
8	Jebba Ts	329.982	99.99	0	60	20
9	BENIN TS	327.912	99.37	-6.1	160	38
10	ALAOJI TS	328.098	99.42	-6.3	180	36
11	SAPELE GS	327.962	99.38	-6.2	0	0
12	ONITSHA TS	330	100	-6.5	160	40
13	AFAM GS	328.098	99.42	-6.3	0	0
14	JEBBA GS	330	100	0	0	0
15	OKPAI GS	330	100	-6.5	0	0
16	GEREGU GS	327.505	99.24	-6.2	0	0
17	AJAOKUTA TS	327.505	99.24	-6.2	40	20
18	OSOGBO TS	328.031	99.4	-1.3	180	40
19	KANO TS	330	100	-11.9	300	45
20	ALADIA TS	327.912	99.37	-6.1	0	0
21	DELTA GS	327.912	99.37	-6.1	0	0
22	GANMO TS	328.689	99.6	-0.6	80	45
23	OMOTOSHO TS	327.048	99.11	-6	0	0
24	EGBIN GS	324.209	98.25	-5.4	0	0
25	IKEJA WEST TS	324.196	98.24	-5.4	420	85
26	NEW HAVEN TS	330	100	-6.7	120	38
27	AKANGBA TS	324.188	98.24	-5.4	120	45
28	SHIRORO GS	327.101	99.12	-5.6	0	0
29	SEKATE TS	323.854	98.14	-5.5	180	53
30	JOS TS	329.713	99.91	-11.4	100	20
31	KADUNA TS	330	100	-9.3	300	45
32	GOMBE TS	330	100	-12.3	80	20
33	MAKURDI TS	330	100	-11.8	50	16
34	YOLA TS	328.119	99.43	-13.3	120	20
Power Loss: P =		43.59 MW	Q = -		538.56MVar	

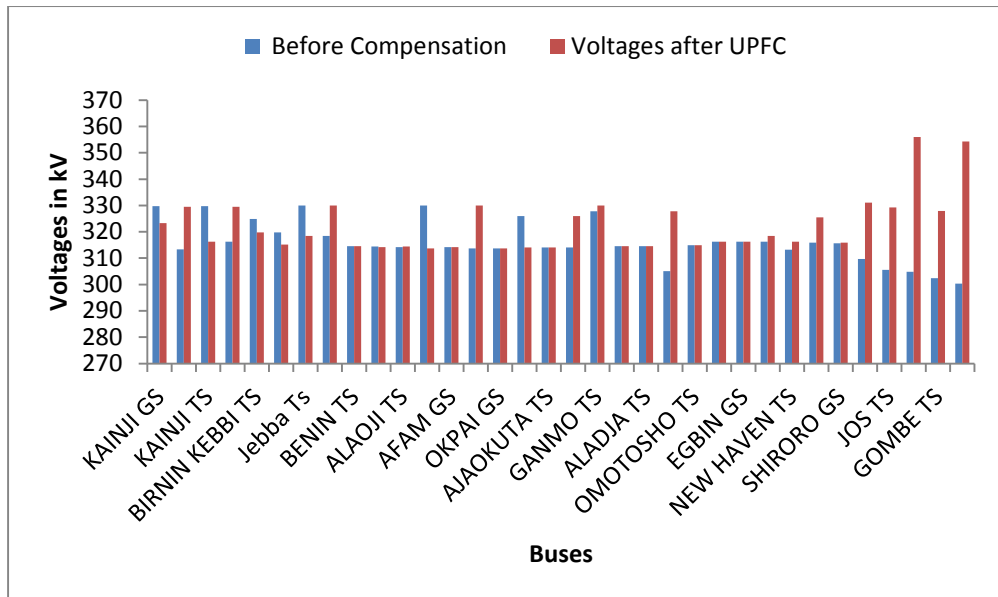


Fig. 4: Graph of Voltage Magnitude against Buses after Compensation with UPFC

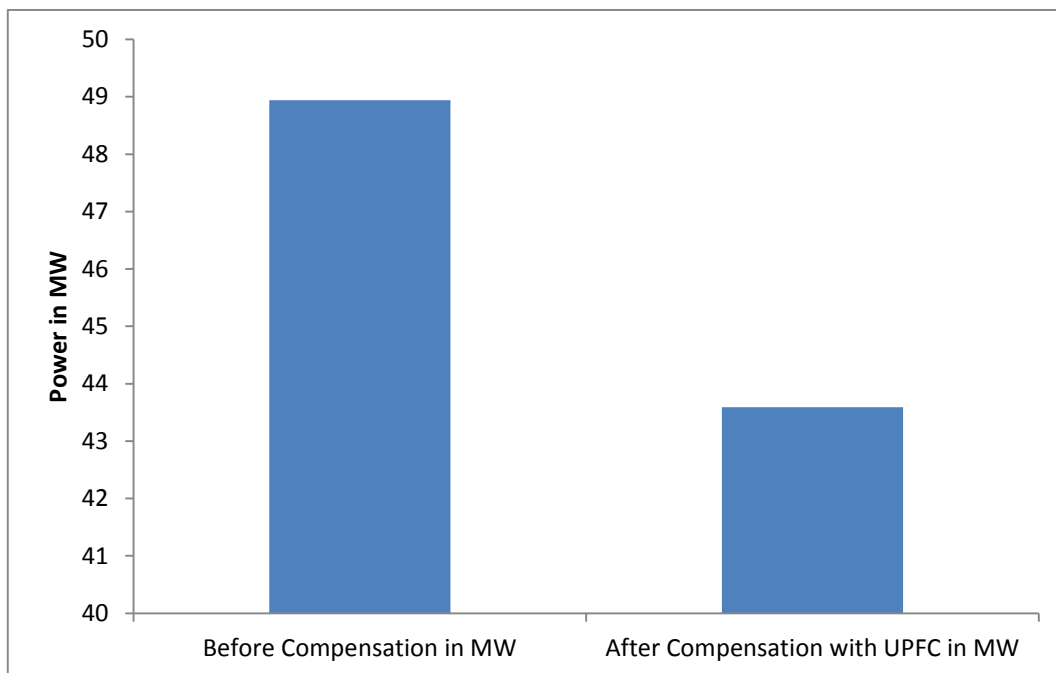


Fig. 5: Graph of Loss Reduction after Compensation with UPFC

IV. CONCLUSION

This paper presents a power flow analysis to determine the effect of UPFC on the power system performance using Nigeria 330 kV, 34-bus power system as a case study. The Simulation was successfully performed under the conditions of steady-state and under the introduction of UPFC. Seven buses were found to have their voltage magnitudes below acceptable values, which include Kano 305.097 kV, New Haven 313.249 kV, Kaduna 309.721 kV, Jos 305.563 kV, Makurdi 304.787 kV, Gombe 304.443 kV and Yola 300.375 kV during the steady-state condition. However, the introduction of UPFC into the modeled power system and simulation in the NEPLAN software revealed compensated voltages at the affected buses of Kano 330 kV, New Haven 330 kV, Jos 329.7 kV, Kaduna 330 kV, Gombe 330 kV, Makurdi 330 kV and Yola 328.59 kV. The total system active power loss was reduced from 49.335 MW to 43.59 MW. This study has established that the deployment of UPFC can positively impact the Nigerian power system network by improving the voltage profile and reducing the total power loss thereby enhancing the electric power transmission system.

REFERENCES

- [1] Sen, K. K. and Sen, M. L. (2004). Introduction to FACTS Controllers, Theory, Modeling and Applications, IEEE press, John Wiley & Sons, inc. New Jersey, Canada.
- [2] Moghavvemi, M. and Faruque, M. O. Effects of Facts Devices on Static Voltage Stability. IEEE ConferenceProceedings, 2, 2000, 357 - 362.
- [3] Rath, S., Sahu, B. P. and Dash, P. Power System Operation and Control Using FACTS Devices. International Journal of Engineering and Technology, 1(5), 2012, 1 - 5.
- [4] Ranjit, K. B. A Review of Benefits of FACTS Devices in Power System. International Journal of Engineering and Advanced Technolgy, 3 (4), 2014, 105 - 108.
- [5] Haddad, S., Haddouche, A. and Bouyeda, H. The Use of FACTS Devices in Disturbed Power Systems – Modeling, Interface and Case Study. International Journal of Computer and Electrical Engineering, 1 (1), 2009, 56 - 60.
- [6] Patel, A. D. A Review of FACTS Devices for the Improvement of Transient Stability. Global Journal of Engineering Science and Researches, 2 (12), 2015, 85 - 89.
- [7] Hemmati, R., Koofigar H., and Ataei, M. Optimal Adaptive controller Based on STATCOM and UPFC. Journal of Electrical Engineering Technology 11(3), 2016, 1921 - 1926.
- [8] Abdulrazzaq, A. A. Improving the Power System Performance using FACTS Devices. Journal of Electrical and Electronics Engineering, 10 (2), 2015, 41 - 49.
- [9] Gautam, K. K. and Tomar, A. K. S. Locating Facts devices in Optimized manner in Power System by means of Sensitivity Analysis, International Journal of Engineering Research and Application, 7 (3), 2017, 75 - 80.
- [10] Jokojeje, R. A., Adejumobi, I. A., Mustapha, A. O. and Adebisi, O. I. Application of Static Synchronous Compensator (STATCOM) in Improving Power System Performance: A Case Study of the Nigeria 330 kV Electricity Grid, Nigerian Journal of Technology, 34(3), 2015, 564 - 572.
- [11] Acha, E., Claudio, R. F., Hugo, A. and Cesar, A. (2004). FACTS – Modeling and Simulation in Power Networks, John Wiley & sons Ltd, West Sussex, England.
- [12] Seifi, A., Sasan, G. M. and Amin, M. S. (2010). Power Flow Study and Comparison of FACTS: Series (SSSC), Shunt (STATCOM) and Shunt-Series (UPFC), The Pacific Journal of Science and Technology, 11(1): 129 – 137.
- [13] Transmission Company of Nigeria Control Centre, Osogbo, South Western, Nigeria. (2013)